




ORIGINAL ARTICLE

Functional assessment of a novel biallelic *MYH3* variation causing CPSKF1B (contractures, pterygia, and spondylarcarpotarsal fusion syndrome1B)

Qing-bing He¹ | Cai-hong Wu² | Dong-lan Sun^{3,4} | Jia-yu Yuan¹ | Hua-ying Hu⁵  | Kai Yang^{6,7}  | Wen-qi Chen^{3,4}  | You-sheng Yan^{6,7} | Guang-yue Yin² | Jing Zhang^{3,4}  | Ya-zhou Li¹

¹Department of Pediatric Orthopaedics, The Third Hospital of Hebei Medical University, Shijiazhuang, Hebei, China

²Department of Clinical Laboratory, Hebei Petrochina Central Hospital, Langfang, China

³Prenatal Diagnosis Center, Shijiazhuang Obstetrics and Gynecology Hospital, Shijiazhuang, China

⁴Hebei Key Laboratory of Maternal and Fetal Medicine; Shijiazhuang Key Laboratory of Reproductive Health, Shijiazhuang, China

⁵Birth Defects Prevention and Control Technology Research Center, Medical Innovation Research Division of Chinese PLA General Hospital, Beijing, China

⁶Prenatal Diagnosis Center, Beijing Obstetrics and Gynecology Hospital, Capital Medical University, Beijing, China

⁷Beijing Maternal and Child Health Care Hospital, Capital Medical University, Beijing, China

Correspondence

Ya-zhou Li, Department of Pediatric Orthopaedics, The Third Hospital of Hebei Medical University, 139 Ziqiang Road, Shijiazhuang, Hebei 050051, China.

Email: lyz_hbsy@126.com

Jing Zhang, Prenatal Diagnosis Center, Shijiazhuang Obstetrics and Gynecology Hospital; Hebei Key Laboratory of Maternal and Fetal Medicine; Shijiazhuang Key Laboratory of Reproductive Health, 16 Tangu-North Street, Shijiazhuang, Hebei 050011, China.

Email: zhangjing_hbyd_81@126.com

Funding information

the Hebei Natural Science Foundation Precision Medicine Joint Fund Cultivation Project, Grant/Award Number: H2021206242; the Science and Technology Research and Development Program of Langfang, Grant/Award Number: 2019013008

Abstract

Background: The *MYH3*-associated myosinopathies comprise a spectrum of rare neuromuscular disorders mainly characterized by distal arthrogryposis with or without other features like pterygia and vertebrae fusion. CPSKF1B (contractures, pterygia, and spondylarcarpotarsal fusion syndrome1B) is the only known autosomal recessive *MYH3*-associated myosinopathy so far, with no more than two dozen cases being reported.

Materials and Methods: A boy with CPSKF1B was recruited and subjected to a comprehensive clinical and imaging evaluation. Genetic detection with whole-exome sequencing (WES) was performed on the patient and extended family members to identify the causative variation. A series of in silico and in vitro investigations were carried out to verify the pathogenicity of the two variants of the identified compound heterozygous variation.

Results: The patient exhibited moderate CPSKF1B symptoms including multi-articular contractures, webbed neck, and spondylarcarpotarsal fusion. WES detected a compound heterozygous *MYH3* variation consisting of two variants, namely NM_002470.4: c.3377A>G; p. (E1126G) and NM_002470.4: c.5161-2A>C. It was indicated that the NM_002470.4: c.3377A>G; p. (E1126G) variant mainly

Qing-bing He, Cai-hong Wu, and Dong-lan Sun equal contributors of this study.

This is an open access article under the terms of the [Creative Commons Attribution-NonCommercial-NoDerivs](https://creativecommons.org/licenses/by-nc-nd/4.0/) License, which permits use and distribution in any medium, provided the original work is properly cited, the use is non-commercial and no modifications or adaptations are made.

© 2024 The Authors. *Molecular Genetics & Genomic Medicine* published by Wiley Periodicals LLC.

impaired the local hydrogen bond formation and impacted the TGF- β pathway, while the NM_002470.4: c.5161-2A>C variant could affect the normal splicing of pre-mRNA, resulting in the appearance of multiple abnormal transcripts.

Conclusions: The findings of this study expanded the mutation spectrum of CPSKF1B, provided an important basis for the counseling of the affected family, and also laid a foundation for the functional study of *MYH3* mutations.

KEYWORDS

contractures, pterygia, and spondylocarpotarsal fusion syndrome-1B, distal arthrogyriposis, functional assessment, *MYH3* gene, whole-exome sequencing

1 | INTRODUCTION

Contractures, pterygia, and spondylocarpotarsal fusion syndrome-1B (CPSFS1B, MIM#618469), belonging to the spondylocarpotarsal synostosis syndrome (SCTS) spectrum, is a recently defined recessive myosinopathy characterized by contractures of proximal and distal joints, pterygia involving the neck, elbows, fingers, and/or knees, and variable vertebral, carpal, and tarsal fusions; inter- and intra-familial variability has been observed (Cameron-Christie et al., 2018). Patients with this disorder often exhibit significant scoliosis and limited mobility. To date, only six studies with less than 20 patients involving with CPSF1B have been reported (Cameron-Christie et al., 2018; Dahan-Oliel et al., 2021; Hakonen et al., 2020; Kamien et al., 2022; Thiffault et al., 2019; Zhao et al., 2022), which keeps the characteristic spectrum, natural clinical course, and pathogenesis of this disease still far from well-known.

The pathogenic gene for CPSFS1B, *MYH3* (myosin heavy chain 3, MIM*160720), is also responsible for the dominant isoform of this condition, CPSFS1A (MIM#178110) (Chong et al., 2015), and for both of the 2A (DA2A, Freeman–Sheldon syndrome, MIM#193700) and 2B3 (DA2B, Sheldon–Hall syndrome, MIM#618436) (Toydemir et al., 2006) subtypes of distal arthrogyriposis (DA). *MYH3* gene, located at chromosome 17p13.1 and spanning a 49 kb genomic region, encodes the heavy chain of embryonic myosin, a muscular protein composed of a globular motor domain attached to a long coiled-coil rod by a short neck and a hinge region (Yoon et al., 1992). *MYH3* is mainly expressed in embryonic development during the first and second trimester, as well in the adult regenerative distal muscle tissue (Racca et al., 2015; Whalen et al., 1981). So far, approximately 60 variants of various types in *MYH3* associated with the generalized DA spectrum (including CPSFS1A/B) have been identified (<https://www.hgmd.cf.ac.uk/>; pro v2021.10); yet, a fine genotype–phenotype association is only emerging, but not

fully established (Beck et al., 2014; Carapito et al., 2016; Zhao et al., 2022). In a previous study, we reported a CPSFS1A case caused by a novel pathogenic variant in *MYH3*, and attempted to generalize the relationship between *MYH3* variations in different domains and disease typing (Zhang et al., 2020). Yet further functional verification studies need to be performed so as to elucidate this relationship.

In the present study, we report on a case of moderate CPSFS1B in a boy and the causative *MYH3* variation he carried. In order to clarify the particular impact of the two variants making up this novel compound heterozygous variation, a set of in vitro experiments was carried out. Meanwhile, we analyzed the interspecies conservation and structural alteration of the amino acid associated with the novel missense variant using in silico methods to support its pathogenicity. Our findings will benefit the establishment of the relationship between the effects of various *MYH3* variants and the resulting phenotypes.

2 | MATERIALS AND METHODS

2.1 | Subjects and clinical evaluation

This study was prospectively reviewed and approved by the Ethics Committee of the Third Hospital of Hebei Medical University (approval No. KE-2022-129-1), and informed consent was signed by all participants. All procedures performed in studies involving human participants were in accordance with the Declaration of Helsinki 1964 and its later amendments or comparable ethical standards.

In Aug 2020, an 8-year-old boy was referred to our center due to multiple joint contracture and limited mobility. Basic clinical evaluation and imaging were performed. We then did a follow-up visit in Nov 2022 to assess disease progression.

2.1.1 | Genetic detection

Genomic DNA was extracted from peripheral blood samples of the patient, his parents and expanded family members using QIAamp DNA Blood Mini kit (Qiagen, Dusseldorf, Germany). Chromosomal microarray analysis (CMA) was performed using Affymetrix CytoScan 750K platform according to manufacturer's standard procedure (Affymetrix Inc., Santa Clara, CA, USA).

Trio-whole exome sequencing was employed to detect the sequence variants in the sample from the proband, as described in our previous study (Yang et al., 2019). In brief, the enrichment of the exonic region sequences was conducted by the Sure Select Human Exon Sequence Capture Kit (Agilent, USA). The DNA libraries were screened using quantitative PCR, the size, distribution, and concentration of which were determined using Agilent Bioanalyzer 2100 (Agilent, Palo Alto, CA, USA), and was massively parallel-sequenced using the Illumina Novaseq6000 platform. The sequencing raw reads (quality level $Q_{30\%} > 90\%$) were aligned to the human reference genome [hg19/GRCh37] in Burrows–Wheeler Aligner tool. The third-party software GATK (<https://software.broadinstitute.org/gatk/>) and the Verita Trekker® Variants Detection system (Berry Genomics, China) were employed for variant calling. Variants with lower quality (read depth $< 10\times$, allele fraction $< 30\%$) were eliminated. Subsequently, the annotation tools, ANNOVAR v2.0 (Wang et al., 2010) and Enliven® Variants Annotation Interpretation systems (Berry Genomics, Beijing, China), were used to provide information for the establishment of the criteria of the common guidelines provided by the American College of Medical Genetics and Genomics (ACMG) (Richards et al., 2015). All variants were filtered through population databases including the 1000 Genomes Project (1000G), Exome Aggregation Consortium (ExAC), and gnomAD only those variants with population frequencies less than 1/1000 in all databases were counted. To maximize clinically diagnostic yield the known pathogenic variants from HGMD pro v2019 (Human Gene Mutation Database) were also retained for further evaluation. The Revel score (for pathogenicity prediction; with ≥ 0.700 as the threshold) (Ioannidis et al., 2016) was also utilized.

As a confirmatory assay, Sanger sequencing was performed with the 3500DX Genetic Analyzer (Applied Biosystems, Thermofisher, LA, CA, USA).

Functional assessment on the MYH3: NM_002470.4: c.3377A>G; p. (E1126G) variant

The evolutionary conservation of amino acid (AA) affected by the missense variant, MYH3: NM_002470.4: c.3377A>G; p. (E1126G), was analyzed using MEGA7 (<http://www.megasoftware.net>) with default parameters.

We also used the Alphafold online program (<https://alphafold.ebi.ac.uk/>), with default parameters, to model and compare the structures of wild-type (WT) and NM_002470.4: c.3377A>G; p. (E1126G) mutant (MT) proteins.

To assess the specific impact of the MYH3: NM_002470.4: c.3377A>G; p. (E1126G) variant, we conducted a further in vitro functional study by cell transfection and Western blotting (WB). First, we constructed the expression vectors of the WT and NM_002470.4: c.3377A>G mutant (MT) of MYH3 cDNA (NM_002470.4, segment size of 5847 bp) using the pcDNA3.1(+) plasmid backbone. Then, we commercially obtained the HEK293 (human embryonic kidney) cell lines and transfected them with the above vectors, respectively. After 48 h, the cells were collected, and the protein was extracted using the RIPA lysis buffer. Next, the extracted proteins were separated on 8% or 10% SDS-PAGE and then electro-transferred to a PVDF membrane (Millipore, Boston, Massachusetts, USA). After blocking the membranes using 5% milk in TBS for 2 h, the membranes were incubated overnight with primary antibodies at 4°C. The antibodies used were anti-heavy chain myosin/MYH3 antibody (ab124205, Abcam, Cambridge, UK), anti-P38 antibody (ab182453, Abcam, Cambridge, UK), anti-P-P38 antibody (ab170099, Abcam, Cambridge, UK), anti-SMAD3 antibody (ab84177, Abcam, Cambridge, UK), anti-P-SMAD3 antibody (ab52903, Abcam, Cambridge, UK). The next day, the PVDF membrane was washed and reacted with HRP-labeled secondary antibodies (611-1302, Rockland, Pottstown, USA) for 30 minutes. The blots were detected through ECL (enhanced chemiluminescence) using FuazonFx (VilberLourmat, Paris, France). The blot images were captured and processed using FusionCapt Advance Fx5 software (VilberLourmat, Paris, France). All experiments were performed in triplicate.

Functional assessment on the MYH3: NM_002470.4: c.5161-2A>C

Splice site prediction algorithms of DANN (Quang et al., 2015) and dbNSFP v3.0 (Liu et al., 2016) indicated that the MYH3: NM_002470.4: c.5161-2A>C variant would be deleterious. Therefore, to assess the impact of this variant on RNA splicing, we performed another set of in vitro experiments. In short, minigene expression plasmids containing the Exon35-Exon37 segment of either the MYH3 (NM_002470.4) wild-type (WT) or the NM_002470.4: c.5161-2A>C mutant (MT) were constructed with a commercially designed expression backbone, pMini-CopGF (concise process diagram see [Figure 4a](#)). Subsequently, HEK293 cells were cultured and transfected by either of these plasmids, respectively. Forty-eight hours later, the cells were collected. Total RNA is extracted from cultured cells according to the

RNA kit II (Omega, Georgia, USA) manufacturer's operating manual. Check the concentration and quality of total RNA using the NanoDrop 2000 spectrophotometer. The mRNA was then reverse transcribed into cDNA by using a PrimeScript RT reagent kit (Takara Bio, Shiga, Japan). Subsequently, particular impact on mRNA splicing was analyzed via PCR fragment amplification, AGE (agarose gel electrophoresis), and Sanger sequencing; the primer sequences used for PCR and sequencing were as follows: MiniRT-F, 5'-GGCTAACTAGAGAACCCACTGCTTA-3'; MYH3-RT-R, 5'-CCTGGTCTCCAGTTTCTGGATCT-3', with TM temperature at 60°C.

3 | RESULTS

3.1 | Clinical indications

The patient was born to a non-consanguineous Chinese couple at full term with normal Apgar scores. He presented mainly with multiarticular limitation, especially in both knees and bimanual joints when he first visited our center. Based on physical examination, this patient had a short wide neck with limited range of motion, a short trunk with pectus carinatum and barrel-shaped chest, sloping shoulders with preserved mobility. In addition, he had moderate neck pterygia. He also has a mild facial deformity, including triangular face with apparently low-set

ears, thick, and slightly arched eyebrows. When the patient was followed up at the age of 10, he showed significant aggravation of interphalangeal joint contracture in both hands and slight aggravation of joint contracture in both knees, presenting with flexion state. Bilateral shoulders were obviously not balanced, and X-ray examination indicated increased scoliosis, fusion of vertebrae, and atlantoaxial fusion. Figure 1 includes the appearance and X-ray images of the patient.

For this patient, continued clinical attention is necessary, particularly in terms of his mobility and vertebral abnormalities. The patient received follow-up in the pediatric Department of Orthopedics of the Third Hospital of Hebei Medical University. The current relevant treatment is conservative treatment and close follow-up. The parents were referred to the Prenatal Diagnosis Center of Shijiazhuang Obstetrics and Gynecology Hospital, for any future pregnancy of the couples in this study, the recurrent risk of CPSKF1B condition would be 25%. Given such circumstances, the couples were informed of reproductive options such as prenatal testing and pre-implantation genetic diagnosis (PGD).

3.2 | Genetic findings

The CMA result was normal, meaning that no CNV (copy number variation) with clinical

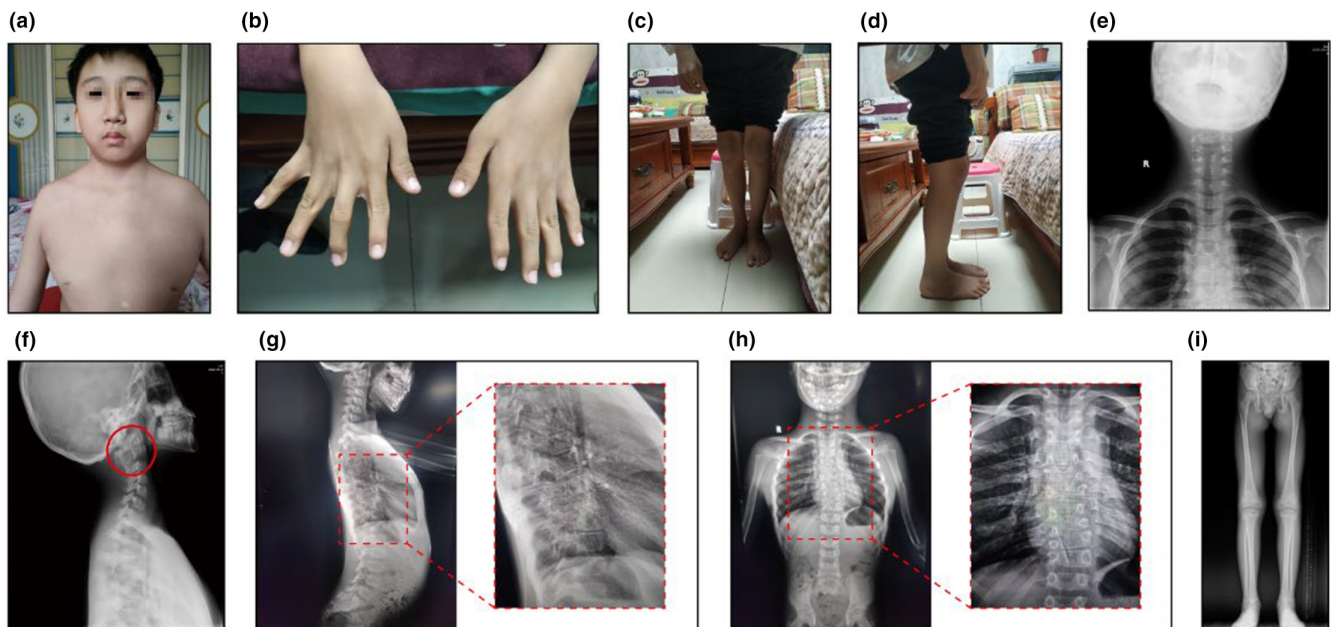


FIGURE 1 The clinical manifestations of the proband in this study. (a) A frontal view of the patient: triangular face, low-set ears, thick and slightly arched eyebrows, webbed neck, barrel-shaped chest, and sloping shoulders. (b) Hands: interphalangeal joint contracture. (c) and (d) The front and side of the lower limbs: flexion state in knees. (e) and (f) X-ray of the front and side of the cervical vertebra: atlantoaxial fusion (red circle). (g) and (h) X-ray of the front and side of the trunk: scoliosis, fusion of vertebrae. (i) X-ray of the front side of the lower limb: no significant abnormality.

significance was detected. WES identified a compound heterozygous variation in *MYH3* consisting of two variants, namely NC_000017.10:g.10541712T>C; NM_002470.4: c.3377A>G; p. (E1126G) and NC_000017.10:g.10535055T>G; NM_002470.4:c.5161-2A>C. Familial validation by Sanger sequencing revealed the variants occurred in trans in the proband and were inherited from other members of the expanded family (Figure 2a,b). According to the ACMG criteria, the pathogenicity of the two variants was interpreted as follows: Uncertain for NM_002470.4: c.3377A>G; p. (E1126G), with evidences of PM2+PM3+PP3; Likely pathogenic for NM_002470.4: c.5161-2A>C, with evidences of PVS1+PM2. The Revel score of NM_002470.4: c.3377A>G; p. (E1126G) variant was 0.851 (damaging).

3.2.1 | The impact of *MYH3*: NM_002470.4: c.3377A>G; p. (E1126G) variant

The MEGA7 program indicated that the *MYH3*: E1126 residue maintained highly conserved across species (Figure 3a). In terms of the structural effect, it was demonstrated that p.E1126G mainly affected the local hydrogen bond formation (Figure 3b; upper red block, WT; lower

red block, mutant). To be specific, in the wild type (WT) model, the E1126 site was hydrogen bonded to R1130 and E1122; the hydrogen bond between E1126 and R1130 existed inside and outside the β -helix, and the hydrogen bond between E1126 and E1122 existed inside the β -helix. While in the mutant (MT) model, although G1126 was still hydrogen-bonded to R1130 and E1122, the hydrogen bonding between G1126 and R1130 outside the β -helix was absent, leaving only the hydrogen bonding inside the β -helix.

The WB result indicated that there was no significant difference in *MYH3*, *SMAD3*, P-*SMAD3*, and *P38* expression in the sample from the Mut as compared to the WT (Figure 3c,d). Phosphorylation level of *P38* was significantly decreased in the sample from the Mut sample as compared to the control (Figure 3c,d).

3.2.2 | The impact of *MYH3*: NM_002470.4: c.5161-2A>C variant on splicing

According to the AGE result of each PCR amplicon, the WT cells could produce the targeted 572-bp product, while intriguingly, the NM_002470.4: c.5161-2A>C mutant (MT) cells produced multiple products with various band sizes (Figure 4b). After analysis with the

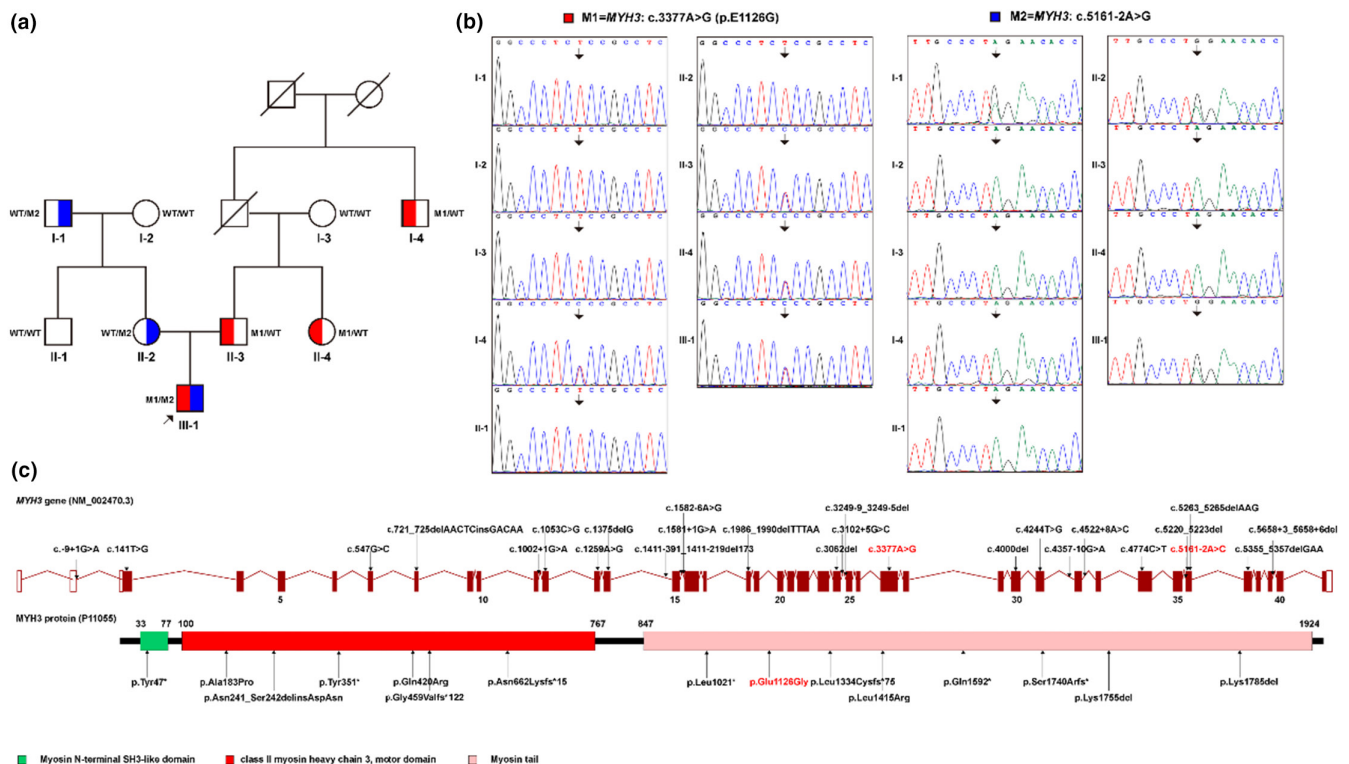


FIGURE 2 Genetic findings. (a) The pedigree diagram and variant carrying status of this family. The red and blue blocks refer to the two variants, respectively, which correspond to (b). (b) Sanger sequencing results of the two variants (*MYH3*: NM_002470.4: c.3377A>G; p. (E1126G) and NM_002470.4: c.5161-2A>C) in all subjects. (c) All the 26 *MYH3* variants causing CPSFS1B reported to date are labeled in gene and protein pattern diagrams. Red fonts refer to the two variants detected in this study.

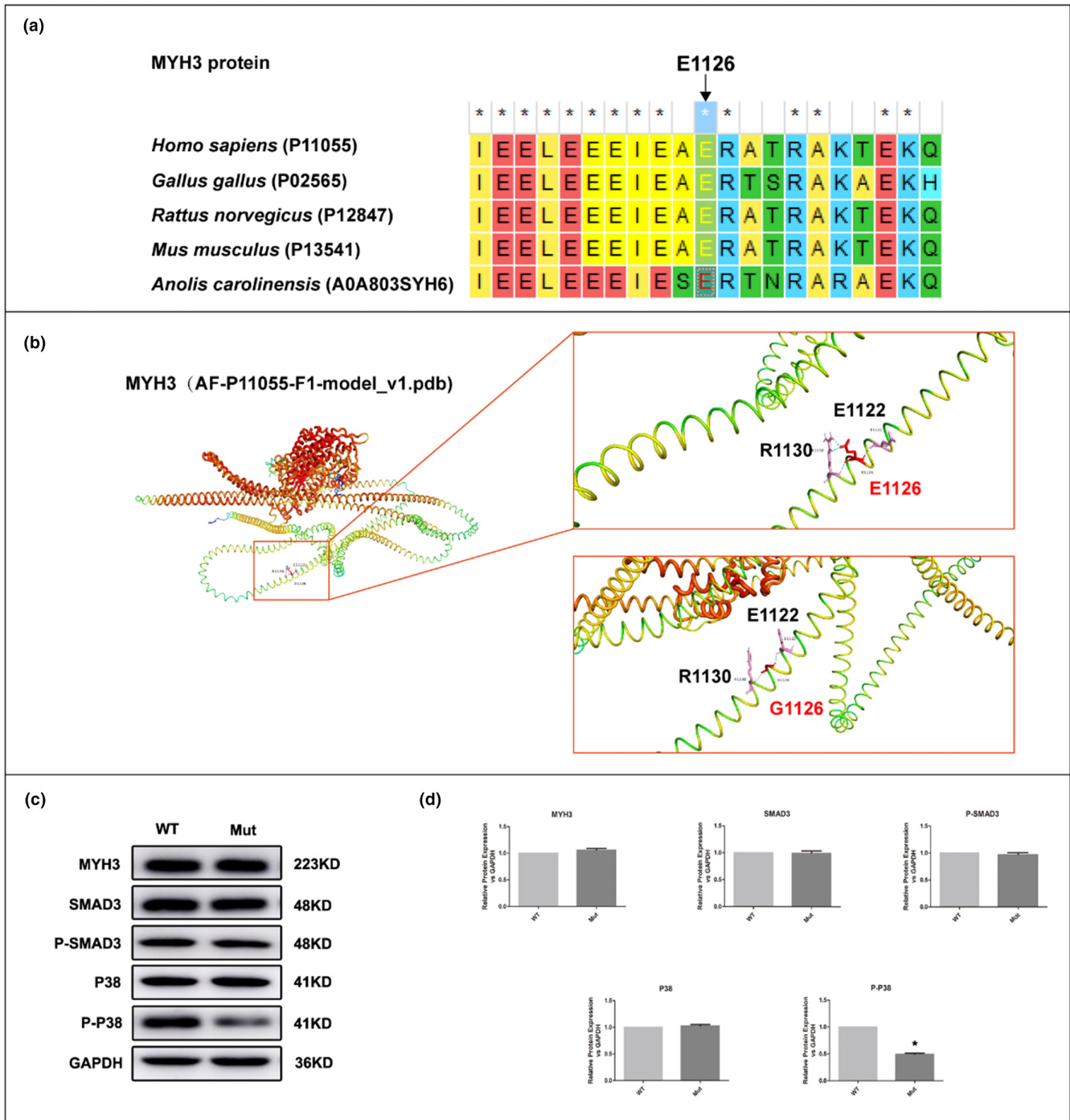


FIGURE 3 Analysis results of the *MYH3*: NM_002470.4: c.3377A>G; p. (E1126G) variant. (a) The interspecies conservation of *MYH3*: E1126 residue. (b) The modeled structures of the WT (upper red block) and Mutant (lower red block). Dotted yellow lines represent the hydrogen bonds. (c) Expression of *MYH3* and proteins in TGF- β signaling pathway: WB results of *MYH3*, *SMAD3*, *P-SMAD3*, *P38*, and *P-P38* expression in WT and the Mut samples. (d) Quantitative analysis of *MYH3*/GAPDH, *SMAD3*/GAPDH, *p-SMAD3*/GAPDH, *P38*/GAPDH, and *P-P38*/GAPDH between the WT and the Mut. All data are expressed as Mean \pm SEM from three independent experiments. In all analyses, * p < 0.05 compared to the corresponding controls was considered the threshold of significance.

corresponding Sanger sequencing results, we determined that the sizes of 3 of them were 446, 564, and 648 bp, respectively (Figure 4c). Specifically speaking, this variant caused three major transcriptional abnormalities: (a)

NM_002470.4:c.5161_5286del, meaning the 126-bp product of Exon36 was completely absent; (b) NM_002470.4:c.5161_5168delAACACCAG, an 8-bp product in Exon36 was lost; (c) NM_002470.4:c.5161-1_5161-76ins, a complete

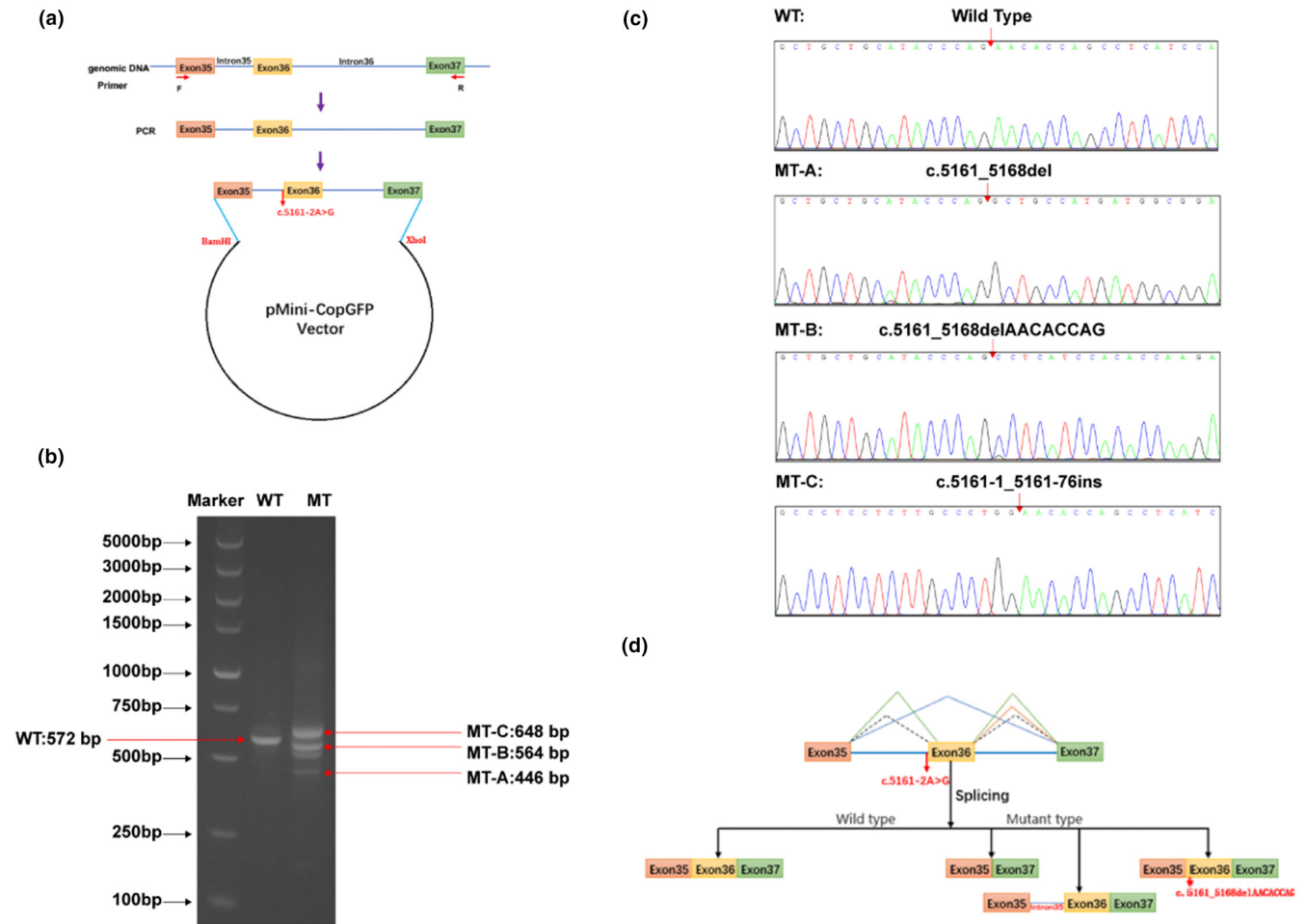


FIGURE 4 Minigene analysis results of the *MYH3*: NM_002470.4:c.5161-2A>C variant. (a) A concise process diagram of the construction of expression plasmids carrying the WT or NM_002470.4:c.5161-2A>C mutant (MT) segments. (b) AGE results of the PCR products. (c) Sanger sequencing results of the WT targeted product and three mutant products (MT-A, MT-B, and MT-C). (d) The schematic of abnormal splicing induced by the *MYH3*: NM_002470.4:c.5161-2A>C variant.

retention of the 76-bp Intron35. The corresponding splicing variation pattern schematic is shown in [Figure 4d](#).

4 | DISCUSSION

Myosins constitute a large superfamily of proteins, which convert chemical energy, through ATP hydrolysis, to mechanical force for diverse cellular movements, such as cell migration and muscle contraction (Sellers, 2000; Yoon et al., 1992). The class II myosin forms the filaments in muscle and non-muscle cells as a hexameric protein complex, consisting of two myosin heavy chain (MyHC) subunits and two pairs of non-identical light chain subunits (He & Gu, 2017). There are several MyHC isoforms encoded by different MYH genes in human, which have been found to be associated with various congenital disorders named myosinopathies (He & Gu, 2017; Tajsharghi & Oldfors, 2013). Among them, the myosinopathies caused

by *MYH3* mutations are mainly manifested by distal arthrogyriposis, yet strong clinical and genetic heterogeneity exhibit in them (Kimber et al., 2012).

The autosomal recessive *MYH3*-associated myosinopathy, CPSFS1B was recognized as spondylcarpotarsal synostosis syndrome (Cameron-Christie et al., 2018). Given how little has been reported about this condition, the full picture remains elusive. From a clinical point of view, this disease needs to be differentiated from many other diseases with similar symptoms, such as its AD homolog, CPSFS1A, and the EVMPs (Escobar variant multiple pterygium syndromes) (Hakonen et al., 2020; Vogt et al., 2012); it thus highlights the need of utilizing high-throughput genetic testing technology. And with more and more *MYH3* biallelic variations being detected in CPSFS1B patients, it increasingly defines the uniqueness of this disease (Zhao et al., 2022). We summarized all the 26 reported *MYH3* variants causing CPSFS1B to date, and included them in [Table 1](#), which were also labeled in the

TABLE 1 The reported recessive genetic variants detected in *MYH3* gene (cited from HGMD database^a and recent literature).

No.	Genomic coordinates	Reference base(s)	Variant base(s)	HGVS ^b description (NM_002470.3)	Protein alteration	Reference (PMID ^c)
1	chr17:10559406-10559406	C	T	c.-9+1G>A	splicing	29805041
2	chr17:10558241-10558241	A	C	c.141T>G	p.Tyr47*	29805041
3	chr17:10552989-10552989	C	G	c.547G>C	p.Ala183Pro	34440395
4	chr17:10551884-10551888	GAGTT	TTGTC	c.721_725delAACTC insGACAA	p.Asn241_Ser242 delinsAspAsn	29805041
5	chr17:10549245-10549245	C	T	c.1002+1G>A	splicing	35169139
6	chr17:10549112-10549112	G	C	c.1053C>G	p.Tyr351*	32902138
7	chr17:10547902-10547902	T	C	c.1259A>G	p.Gln420Arg	35484034
8	chr17:10547703-10547703	C	del	c.1375delG	p.Gly459Valfs*122	35484034
9	chr17:10546532-10546704	TCTGGGCATC TCTTGTGTA CTTTATTTT GTAGTTACTC TTCAATGTGCCA	del	c.1411-391_1411-219 del173	splicing	29805041
10	chr17:10546142-10546142	C	T	c.1581+1G>A	splicing	29805041
11	chr17:10546046-10546046	T	C	c.1582-6A>G	splicing	35169139
12	chr17:10544659-10544663	TTAAA	del	c.1986_1990delTTTAA	p.Asn662Lysfs*15	29805041
13	chr17:10542655-10542655	A	del	c.3062del	p.Leu1021*	35169139
14	chr17:10542610-10542610	C	G	c.3102+5G>C	splicing	32902138
15	chr17:10542285-10542289	GAAGA	del	c.3249-9_3249-5del	splicing	35169139
16	chr17:10541712-10541712	T	C	c.3377A>G	p.Glu1126Gly	this study
17	chr17:10538856-10538856	G	del	c.4000del	p.Leu1334Cysfs*75	35169139
18	chr17:10538269-10538269	A	C	c.4244T>G	p.Leu1415Arg	35169139
19	chr17:10537509-10537509	C	T	c.4357-10G>A	splicing	35169139
20	chr17:10537326-10537326	T	G	c.4522+8A>C	splicing	35484034
21	chr17:10535975-10535975	G	A	c.4774C>T	p.Gln1592*	35484034
22	chr17:10535055-10535055	T	G	c.5161-2A>C	splicing	This study
23	chr17:10534991-10534994	CTCA	del	c.5220_5223del	p.Ser1740Arfs*	35169139
24	chr17:10534949-10534951	CTT	del	c.5263_5265delAAG	p.Lys1755del	30008475
25	chr17:10533705-10533707	TTC	del	c.5355_5357delGAA	p.Lys1785del	30008475
26	chr17:10533153-10533156	ACTT	del	c.5658+3_5658+6del	splicing	35169139

^aHGMD, The Human Gene Mutation Database (<http://www.hgmd.cf.ac.uk/ac/index.php>);

^bHGVS, Human Genome Variation Society (<http://www.hgvs.org/>);

^cPMID, PubMed reference ID (<https://pubmed.ncbi.nlm.nih.gov/>).

gene and protein schematics in Figure 2c. From the types of variants and their distribution, it is not enough to conclude a certain rule; therefore, necessary functional experiments can help to determine the effects of each variant.

In terms of the *MYH3*: NM_002470.4: c.3377A>G; p. (E1126G) variant, although it could only be interpreted as with uncertain clinical significance from the genetic perspective, subsequent in silico and functional evidences were in favor of its pathogenicity. First, the interspecies conservation of *MYH3*: E1126 residue supported the pathogenicity of *MYH3*: NM_002470.4: c.3377A>G; p. (E1126G) variant,

indirectly. Second, at the intramolecular structural level, with the alteration of hydrogen bonding formation, this variant was expected to most likely affect the stability and normal function of the β -helix in this region (Syamaladevi et al., 2012). Additionally, the variant was located in the coiled coil region of MyHC and could potentially disrupt its connection to sarcoid or other sarcoid proteins (He & Gu, 2017). Inhibition of TGF β signaling can result in muscle cell hypertrophy (Burks & Cohn, 2011). Third, Zieba et al. once showed that the truncated mutation c.2699delT of *MYH3* resulted in the downregulation of P-P38, which

affected the TGF- β signaling pathway, may affect phenotype by inducing inappropriate muscle hypertrophy and function (Zieba et al., 2017). Our results suggested that NM_002470.4: c.3377A>G; p. (E1126G) had a similar effect. Interestingly, yet, NM_002470.4: c.3377A>G; p. (E1126G) did not produce the dominant effect that led directly to symptoms. The deep reason for this may be related to the specific type and location of different variants, which needs further elucidation.

As for the *MYH3*: NM_002470.4:c.5161-2A>C variant, although we had predicted that it would have an impact on splicing, we did not expect such complex multiple transcripts to be produced. This is most likely due to the fact that this variant overwhelmed the dominant splicing acceptor site and allowed other cryptic acceptors to function, which is probably related to the change of mRNA secondary structure (Rubtsov, 2016). The fact that this variant failed to result in an autosomal dominant phenotype may have something to do with its ability to produce some residual functional protein. But further experiments are needed to confirm this hypothesis.

In summary, in this study, we conducted a thorough clinical evaluation and imaging examination of a boy with CPSKF1B condition, and identified its pathogenic variation by whole-exome sequencing. Subsequently, we performed primary functional studies on the two variants in this compound heterozygous variation of *MYH3* gene to verify its pathogenicity and clarify its mechanism. Our findings extend the mutation spectrum of *MYH3*-associated recessive CPSKF1B, provide solid basis for counseling the affected families, and shed light on the establishment of the genotype–phenotype association of *MYH3* myosinopathy.

AUTHOR CONTRIBUTIONS

Q.-b.H., J.Z., and Y.-z.L. designed and supervised this study. J.-y.Y. and Y.-z.L. recruited the case and conducted the clinical evaluation. C.-h.W. and D.-l.S. performed the imaging examination. K.Y., J.Z., Y.-s.Y., and H.-y.H. performed the genetic and data analysis. C.-h.W. and G.-y.Y. carried out the in silico analysis. J.-y.Y., C.-h.W., and D.-l.S. conducted the in vitro study. J.-y.Y., C.-h.W., and D.-l.S. wrote the manuscript, and all co-authors reviewed it and approved its submission. All authors have read and agreed to the published version of the manuscript.

ACKNOWLEDGMENTS

We acknowledge all the participants in this study.

FUNDING INFORMATION

This work was supported by the Hebei Natural Science Foundation Precision Medicine Joint Fund Cultivation Project (No. H2021206242), and the Science and

Technology Research and Development Program of Langfang (No. 2019013008).

CONFLICT OF INTEREST STATEMENT

Jia-yu Yuan, Cai-hong Wu, Dong-lan Sun, Hua-ying Hu, Kai Yang, Wen-qi Chen, You-sheng Yan, Guang-yue Yin, Jing Zhang, and Ya-zhou Li declare that they have no conflict of interest.

DATA AVAILABILITY STATEMENT

The data that support the findings of this study are openly available in figshare at <https://figshare.com/>, reference number <https://doi.org/10.6084/m9.figshare.24737091>.

ETHICS STATEMENT AND CONSENT TO PARTICIPATE

The samples used in this study were collected with appropriate informed consent and approval of the Ethics Committee of the Third Hospital of Hebei Medical University. The methods used in this study were carried out in accordance with the approved guidelines.

ORCID

Hua-ying Hu  <https://orcid.org/0000-0002-3933-1451>

Kai Yang  <https://orcid.org/0000-0002-7457-3106>

Wen-qi Chen  <https://orcid.org/0000-0002-9304-1965>

Jing Zhang  <https://orcid.org/0000-0002-9957-3372>

REFERENCES

- Beck, A. E., McMillin, M. J., Gildersleeve, H. I., Shively, K. M., Tang, A., & Bamshad, M. J. (2014). Genotype-phenotype relationships in freeman-Sheldon syndrome. *American Journal of Medical Genetics. Part A*, 164A(11), 2808–2813. <https://doi.org/10.1002/ajmg.a.36762>
- Burks, T. N., & Cohn, R. D. (2011). Role of TGF- β signaling in inherited and acquired myopathies. *Skeletal Muscle*, 1(1), 19. <https://doi.org/10.1186/2044-5040-1-19>
- Cameron-Christie, S. R., Wells, C. F., Simon, M., Wessels, M., Tang, C. Z. N., Wei, W., Takei, R., Aarts-Tesselaar, C., Sandaradura, S., Sillence, D. O., Cordier, M. P., Veenstra-Knol, H. E., Cassina, M., Ludwig, K., Trevisson, E., Bahlo, M., Markie, D. M., Jenkins, Z. A., & Robertson, S. P. (2018). Recessive Spondylarcarpotarsal synostosis syndrome due to compound heterozygosity for variants in *MYH3*. *American Journal of Human Genetics*, 102(6), 1115–1125. <https://doi.org/10.1016/j.ajhg.2018.04.008>
- Carapito, R., Goldenberg, A., Paul, N., Pichot, A., David, A., Hamel, A., Dumant-Forest, C., Leroux, J., Ory, B., Isidor, B., & Bahram, S. (2016). Protein-altering *MYH3* variants are associated with a spectrum of phenotypes extending to spondylarcarpotarsal synostosis syndrome. *European Journal of Human Genetics*, 24(12), 1746–1751. <https://doi.org/10.1038/ejhg.2016.84>
- Chong, J. X., Burrage, L. C., Beck, A. E., Marvin, C. T., McMillin, M. J., Shively, K. M., Harrell, T. M., Buckingham, K. J., Bacino, C. A., Jain, M., Alanay, Y., Berry, S. A., Carey, J. C., Gibbs,

- R. A., Lee, B. H., Krakow, D., Shendure, J., Nickerson, D. A., University of Washington Center for Mendelian Genomics, & Bamshad, M. J. (2015). Autosomal-dominant multiple pterygium syndrome is caused by mutations in MYH3. *American Journal of Human Genetics*, 96(5), 841–849. <https://doi.org/10.1016/j.ajhg.2015.04.004>
- Dahan-Oliel, N., Dieterich, K., Rauch, F., Bardai, G., Blondell, T. N., Gustafson, A. G., Hamdy, R., Latypova, X., Shazand, K., Giampietro, P. F., & van Bosse, H. (2021). The clinical and genotypic Spectrum of scoliosis in multiple pterygium syndrome: A case series on 12 children. *Genes (Basel)*, 12(8):1220. <https://doi.org/10.3390/genes12081220>
- Hakonen, A. H., Lehtonen, J., Kivirikko, S., Keski-Filppula, R., Moilanen, J., Kivisaari, R., Almusa, H., Jakkula, E., Saarela, J., Avela, K., & Aittomaki, K. (2020). Recessive MYH3 variants cause “contractures, pterygia, and variable skeletal fusions syndrome 1B” mimicking Escobar variant multiple pterygium syndrome. *American Journal of Medical Genetics. Part A*, 182(11), 2605–2610. <https://doi.org/10.1002/ajmg.a.61836>
- He, Y. M., & Gu, M. M. (2017). Research progress of myosin heavy chain genes in human genetic diseases. *Yi Chuan*, 39(10), 877–887. <https://doi.org/10.16288/j.ycz.17-090>
- Ioannidis, N. M., Rothstein, J. H., Pejaver, V., Middha, S., McDonnell, S. K., Baheti, S., Musolf, A., Li, Q., Holzinger, E., Karyadi, D., Cannon-Albright, L. A., Teerlink, C. C., Stanford, J. L., Isaacs, W. B., Xu, J., Cooney, K. A., Lange, E. M., Schleutker, J., Carpten, J. D., ... Sieh, W. (2016). REVEL: An ensemble method for predicting the pathogenicity of rare missense variants. *American Journal of Human Genetics*, 99(4), 877–885. <https://doi.org/10.1016/j.ajhg.2016.08.016>
- Kamien, B., Clayton, J. S., Lee, H. S., Abeyesuriya, D., McNamara, E., Martinovic, J., Gonzales, M., Melki, J., & Ravenscroft, G. (2022). Bi-allelic MYH3 loss-of-function variants cause a lethal form of contractures, pterygia, and spondylocarpotarsal fusion syndrome 1B. *Neuromuscular Disorders*, 32(5), 445–449. <https://doi.org/10.1016/j.nmd.2022.03.007>
- Kimber, E., Tajsharghi, H., Krokmark, A. K., Oldfors, A., & Tulinius, M. (2012). Distal arthrogyrosis: Clinical and genetic findings. *Acta Paediatrica*, 101(8), 877–887. <https://doi.org/10.1111/j.1651-2227.2012.02708.x>
- Liu, X., Wu, C., Li, C., & Boerwinkle, E. (2016). dbNSFP v3.0: A one-stop database of functional predictions and annotations for human nonsynonymous and splice-site SNVs. *Human Mutation*, 37(3), 235–241. <https://doi.org/10.1002/humu.22932>
- Quang, D., Chen, Y., & Xie, X. (2015). DANN: A deep learning approach for annotating the pathogenicity of genetic variants. *Bioinformatics*, 31(5), 761–763. <https://doi.org/10.1093/bioinformatics/btu703>
- Racca, A. W., Beck, A. E., McMillin, M. J., Korte, F. S., Bamshad, M. J., & Regnier, M. (2015). The embryonic myosin R672C mutation that underlies freeman-Sheldon syndrome impairs cross-bridge detachment and cycling in adult skeletal muscle. *Human Molecular Genetics*, 24(12), 3348–3358. <https://doi.org/10.1093/hmg/ddv084>
- Richards, S., Aziz, N., Bale, S., Bick, D., das, S., Gastier-Foster, J., Grody, W. W., Hegde, M., Lyon, E., Spector, E., Voelkerding, K., Rehm, H. L., & ACMG Laboratory Quality Assurance Committee. (2015). Standards and guidelines for the interpretation of sequence variants: A joint consensus recommendation of the American College of Medical Genetics and Genomics and the Association for Molecular Pathology. *Genetics in Medicine*, 17(5), 405–424. <https://doi.org/10.1038/gim.2015.30>
- Rubtsov, P. M. (2016). Role of pre-mRNA secondary structures in the regulation of alternative splicing. *Molecular Biology*, 50(6), 823–830. <https://doi.org/10.1134/s0026893316060170>
- Sellers, J. R. (2000). Myosins: A diverse superfamily. *Biochimica et Biophysica Acta*, 1496, 3–22.
- Syamaladevi, D. P., Spudich, J. A., & Sowdhamini, R. (2012). Structural and functional insights on the myosin superfamily. *Bioinformatics and Biology Insights*, 6, 11–21. <https://doi.org/10.4137/BBI.S8451>
- Tajsharghi, H., & Oldfors, A. (2013). Myosinopathies: Pathology and mechanisms. *Acta Neuropathologica*, 125(1), 3–18. <https://doi.org/10.1007/s00401-012-1024-2>
- Thiffault, I., Farrow, E., Zellmer, L., Berrios, C., Miller, N., Gibson, M., Caylor, R., Jenkins, J., Faller, D., Soden, S., & Saunders, C. (2019). Clinical genome sequencing in an unbiased pediatric cohort. *Genetics in Medicine*, 21(2), 303–310. <https://doi.org/10.1038/s41436-018-0075-8>
- Toydemir, R. M., Rutherford, A., Whitby, F. G., Jorde, L. B., Carey, J. C., & Bamshad, M. J. (2006). Mutations in embryonic myosin heavy chain (MYH3) cause freeman-Sheldon syndrome and Sheldon-hall syndrome. *Nature Genetics*, 38(5), 561–565. <https://doi.org/10.1038/ng1775>
- Vogt, J., Morgan, N. V., Rehal, P., Faivre, L., Brueton, L. A., Becker, K., Fryns, J. P., Holder, S., Islam, L., Kivuva, E., Lynch, S. A., Touraine, R., Wilson, L. C., MacDonald, F., & Maher, E. R. (2012). CHRNG genotype-phenotype correlations in the multiple pterygium syndromes. *Journal of Medical Genetics*, 49(1), 21–26. <https://doi.org/10.1136/jmedgenet-2011-100378>
- Wang, K., Li, M., & Hakonarson, H. (2010). ANNOVAR: Functional annotation of genetic variants from next-generation sequencing data. *Nucleic Acids Research*, 38, e164. <https://doi.org/10.1093/nar/gkq603>
- Whalen, R. G., Sell, S. M., Butler-Browne, G. S., Schwartz, K., Bouveret, P., & Pinset-Härstöm, I. (1981). Three myosin heavy-chain isozymes appear sequentially in rat muscle development. *Nature*, 292(5826), 805–809. <https://doi.org/10.1038/292805a0>
- Yang, K., Shen, M., Yan, Y., Tan, Y., Zhang, J., Wu, J., Yang, G., Li, S., Wang, J., Ren, Z., Dong, Z., Wang, S., Zhang, M., & Tian, Y. (2019). Genetic analysis in fetal skeletal Dysplasias by trio whole-exome sequencing. *BioMed Research International*, 2019, 1–8. <https://doi.org/10.1155/2019/2492590>
- Yoon, S.-J., Seiler, S. H., Kucherlapati, R., & Leinwand, L. (1992). Organization of the human skeletal myosin heavy chain gene cluster. *PNAS*, 89, 12078–12082.
- Zhang, J., Chen, W. Q., Wang, S. W., Wang, S. X., Yu, M., Guo, Q., & Yu, Y. D. (2020). Identification of a novel pathogenic variant in the MYH3 gene in a five-generation family with CPSFS1A (contractures, pterygia, and Spondylocarpotarsal fusion syndrome 1A). *Molecular Genetics & Genomic Medicine*, 8(10), e1440. <https://doi.org/10.1002/mgg3.1440>
- Zhao, S., Zhang, Y., Hallgrimsdottir, S., Zuo, Y., Li, X., Batkovskytte, D., Liu, S., Lindelöf, H., Wang, S., Hammarsjö, A., Yang, Y., Ye, Y., Wang, L., Yan, Z., Lin, J., Yu, C., Chen, Z., Niu, Y.,

- Wang, H., ... Wu, N. (2022). Expanding the mutation and phenotype spectrum of MYH3-associated skeletal disorders. *NPJ Genomic Medicine*, 7(1), 11. <https://doi.org/10.1038/s41525-021-00273-x>
- Zieba, J., Zhang, W., Chong, J. X., Forlenza, K. N., Martin, J. H., Heard, K., Grange, D. K., Butler, M. G., Kleefstra, T., Lachman, R. S., Nickerson, D., Regnier, M., Cohn, D. H., Bamshad, M., & Krakow, D. (2017). A postnatal role for embryonic myosin revealed by MYH3 mutations that alter TGFbeta signaling and cause autosomal dominant spondylocarpotarsal synostosis. *Scientific Reports*, 7, 41803. <https://doi.org/10.1038/srep41803>

How to cite this article: He, Q.-b., Wu, C.-h., Sun, D.-l., Yuan, J.-y., Hu, H.-y., Yang, K., Chen, W.-q., Yan, Y.-s., Yin, G.-y., Zhang, J., & Li, Y.-z. (2024). Functional assessment of a novel biallelic *MYH3* variation causing CPSKF1B (contractures, pterygia, and spondylocarpotarsal fusion syndrome1B). *Molecular Genetics & Genomic Medicine*, 12, e2401. <https://doi.org/10.1002/mgg3.2401>